Published Online: 2025 August 31

Research Article

Green Synthesis and Antibacterial Activity of Zinc Oxide Nanoparticles Using Rosemary (*Salvia rosmarinus*) Extract

Noor Sabah Khadim [1], Dunya Sabeeh Mohammed [2], Salim Albukhaty [3], Zaidon T. Al-aqbi [4], Fariba Qate [5,*]

[1] Department of Pharmaceutical Chemistry , College of Pharmacy, University of Misan, Maysan, Iraq
[2] Department of Pharmacognosy and Medicinal Plants, College of Pharmacy, University of Misan, Maysan, Iraq
[3] Department of Pharmaceutical Chemistry, College of Pharmacy, University of Manara, Maysan, Iraq
[4] Department of Chemistry, College of Science, University of Misan, Maysan, Iraq
[5] Department of Horticulture Science, Faculty of Agriculture, Shahid Chamran University of Ahvaz, Ahvaz, Iran

[*] ***Corresponding Author:*** Department of Horticulture Science, Faculty of Agriculture, Shahid Chamran University of Ahvaz, Ahvaz, Iran. Email: ghatefariba@gmail.com

Received: 19 July, 2025; **Revised:** 29 July, 2025; **Accepted:** 10 August, 2025

Abstract

Background: Green synthesis by plants is a good alternative to conventional chemical methods, as it eliminates hazardous reagents and reduces environmental impacts.

Objectives: This study aims to green synthesize zinc oxide nanoparticles (ZnO NPs) using rosemary as a natural reductant and stabilizer.

Methods: The characterization of the biosynthesized ZnO NPs was conducted via UV-visible spectroscopy, Fourier transform infrared (FTIR) spectroscopy, X-ray diffraction (XRD), dynamic light scattering (DLS), zeta potential (ZP) analysis, scanning electron microscopy (SEM), and energy dispersive X-ray spectroscopy (EDX). The antibacterial activity was tested against both the representative gram-positive *Staphylococcus aureus* and gram-negative *Escherichia coli* bacteria.

Results: The characterizations identified crystalline ZnO NPs with a hexagonal wurtzite structure and an average crystallite size of 46.14 nm. The DLS revealed a hydrodynamic size of 652.5 nm, coupled with a high negative ZP (-45.4 mV), indicating excellent colloidal stability. The FTIR and EDX results indicated phytochemical residues of rosemary on the surfaces of nanoparticles, thus confirming the dual role of the extract responsible for both reduction and capping. The SEM images revealed geometries ranging from spherical to hexagonally shaped and uniformly distributed, while EDX confirmed elemental purity.

Conclusions: Plant-mediated green synthesis to fabricate functional zinc oxide (ZnO) nanomaterials with excellent antibacterial properties is feasible, as demonstrated in this work. The rosemary-mediated approach offers sustainable avenues for the application of antimicrobial therapy, biomedical devices, and environmental remediation. The dual functionality of rosemary extract as a reducing and stabilizing agent, coupled with synergistic antibacterial action, contributes to the advantages of green synthesis methods for nanotechnology applications.

Keywords: Green Synthesis, Zinc Oxide NPs, Rosemary Extract, Phytochemicals, Zeta Potential, XRD

1. Background

The remarkable growth of nanotechnology drives the development of new materials with diverse physicochemical and biological properties. Among the most studied are zinc oxide nanoparticles (ZnO NPs) (1). The ZnO NPs possess excellent optical, electronic, and antimicrobial properties, making them useful in various fields such as biomedicine, environmental cleanup, and electronics. However, traditional methods for synthesizing ZnO NPs involve hazardous chemicals and energy-intensive processes, raising environmental and biocompatibility concerns. To address these issues, researchers have explored green synthesis methods,

Copyright © 2025, Sabah Khadim et al. This open-access article is available under the Creative Commons Attribution 4.0 (CC BY 4.0) International License (https://creativecommons.org/licenses/by/4.0/), which allows for unrestricted use, distribution, and reproduction in any medium, provided that the original work is properly cited.

How to Cite: Sabah Khadim N, Sabeeh Mohammed D, Albukhaty S, T. Al-aqbi Z, Qate F. Green Synthesis and Antibacterial Activity of Zinc Oxide Nanoparticles Using Rosemary (*Salvia rosmarinus*) Extract. Jundishapur J Nat Pharm Prod. 2025; 20 (4): e164560. https://doi.org/10.5812/jjnpp-164560.

especially those using plant extracts as reducing and stabilizing agents (2).

Rosemary (*Salvia rosmarinus*) extract has become prominent in the eco-friendly production of ZnO NPs, marking a significant advancement in sustainable nanotechnology (3). This Mediterranean herb is rich in phytochemicals, such as terpenes, flavonoids, and phenolic acids. These bioactive compounds naturally act as reducing and stabilizing agents, converting metal ions into nanoparticles and maintaining their stability during synthesis (4). The functional groups in rosemary facilitate efficient nucleation and growth of ZnO NPs without relying on harmful chemicals. This approach aligns with green chemistry principles by reducing environmental harm through limiting toxic reagents and waste. The plant-based extract also improves nanoparticle compatibility for biomedical and pharmaceutical applications (5).

Furthermore, rosemary is readily available and inexpensive, contributing to the economic viability of the synthesis process. The bioactivity of the phytochemicals may also impart antibacterial and antioxidant properties to the ZnO NPs, enhancing their functional potential. Compared to conventional physical and chemical methods of nanoparticle production, green synthesis with rosemary extract offers clear advantages (6).

Traditional approaches often require strong reducing agents, stabilizers, or surfactants that pose environmental and health risks, whereas rosemary extract provides a natural and non-toxic alternative. The process tends to be simpler, with milder reaction conditions and less need for specialized equipment. The phytochemicals in rosemary also improve the colloidal stability of the nanoparticles, as indicated by favorable zeta potential (ZP) measurements. Additionally, green methods consume less energy due to lower operating temperatures and pressures.

The significance of rosemary-mediated green synthesis of ZnO NPs lies in overcoming the limitations of conventional methods and enabling new biological functionalities. These nanoparticles leverage zinc oxide's inherent properties along with rosemary-derived bioactive compounds, showing promise for many applications, especially in antimicrobial and biomedical fields. Overall, green synthesis using rosemary extract promotes a sustainable, efficient, and versatile pathway for producing ZnO NPs, supporting the global goal of environmentally responsible scientific innovation (7).

Much is happening regarding the plant-mediated synthesis of metal oxide nanoparticles, but aspects of all these methods are still not well understood (8). For instance, the understanding of how the phytochemicals work on the nanoparticle nucleation, the organism, growth, or stabilization is not thorough (9). Furthermore, the physicochemical characteristics of green-synthesized ZnO NPs may not have a profound or direct correlation with their biological activity, particularly their antibacterial properties. This study will fill these gaps through systematic research into the synthesis process, detailed characterization, and antibacterial performance of ZnO NPs produced using rosemary extract.

2. Objectives

This study proposes a novel approach toward the green synthesis of ZnO NPs, utilizing rosemary plant extract as both a reducing and capping agent. The scope of the study involves optimizing the synthesis method, conducting structural and surface characterization of the nanoparticles, and assessing antimicrobial activity in both gram-positive and gram-negative bacteria. This work not only advances the understanding of plant mediation in the synthesis of nanoparticles but also demonstrates that rosemary-sourced ZnO NPs can be considered for use as strong antimicrobial agents.

The first section describes the materials and methods for preparing rosemary extract and synthesizing ZnO NPs. Following this, the procedure presents the results of a comprehensive set of characterization studies, including X-ray diffraction (XRD), Fourier transform infrared (FTIR) spectroscopy, UV-visible spectroscopy, field emission scanning electron microscopy (FESEM), energy dispersive X-ray spectroscopy (EDX), dynamic light scattering (DLS), and ZP measurements. The characterization of synthesized nanoparticles for antibacterial activity will then be evaluated and discussed. The article concludes with a summary of key findings and implications for future research and applications.

3. Methods

3.1. Materials

Ciprofloxacin (from Sigma-Aldrich), Mueller-Hinton broth (from Millipore, Merck), and zinc chloride dihydrate ($ZnCl_2 \cdot 2H_2O$, 99.7%, from Merck) were acquired and used as received, without any further purification. Hydrochloric acid (HCl; from Merck) and 1M sodium hydroxide (NaOH; from Sigma-Aldrich) were also used as purchased. Fresh rosemary (*S. rosmarinus*) leaves were collected in October 2024 for this study.

3.2. Collection of Plant Material, Preparation, and Extraction of Rosemary Extract

Fresh leaves of rosemary (*S. Rosmarinus*) were obtained from a cultivated garden in Misan, Iraq, in October 2024. Authentication of the plant material was done by a qualified botanist from the Department of Pharmacognosy and Medicinal Plants, College of Pharmacy, University of Misan, to ensure correct identification of the species. Immediately after collection, the rosemary leaves were washed with double-distilled water to remove dust and surface contaminants. The leaves were then air-dried using sterile paper towels. The washed rosemary leaves were carefully trimmed and chopped into small pieces with a sterilized stainless-steel knife. The prepared plant material was air-dried at room temperature in a shaded, dust-free environment until a constant weight was achieved. Once dry, the leaves were finely powdered with the help of a clean laboratory grinder. For the extraction, about 10 grams of powdered rosemary leaves were mixed with 100 milliliters of double-distilled water at a ratio of 1:10 (w/v). The mixture was homogenized in a laboratory blender for 2 - 3 minutes to ensure uniform extraction of phytochemicals. The slurry was filtered through layers of sterile muslin cloth to remove solid residues and collect the clear aqueous extract. The filtrate was then centrifuged at 5,000 rpm for 10 minutes to further clarify the extract and remove any remaining particulate matter. Thereafter, the supernatant was collected and transferred into sterile storage bottles. The rosemary extract was kept at 4°C for short-term use or at -20°C for long-term preservation until required for subsequent experimental procedures (10).

3.3. Biosynthesis of Zinc Oxide Nanoparticles Using Rosemary (Salvia Rosmarinus) Extract

The green synthesis of zinc oxide (ZnO) nanoparticles was achieved utilizing an aqueous extract of rosemary (*S. Rosmarinus*) leaves, which served as both the reducing and stabilizing agent. Initially, a stock solution of $ZnCl_2{\cdot}2H_2O$ (99.7%; Merck) was prepared by dissolving 2.7 grams of $ZnCl_2{\cdot}2H_2O$ in 200 milliliters of deionized water in a glass beaker. The solution was stirred continuously at room temperature (20±2°C) until the zinc salt was completely dissolved. Separately, an aqueous rosemary extract was prepared as previously described. For the biosynthesis process, 10 milliliters of the prepared rosemary extract were gradually added dropwise to the zinc chloride solution using a burette, while maintaining constant stirring. The reaction mixture was initially kept at 20°C, and then the temperature was increased to 80°C to facilitate the reduction and nucleation of ZnO NPs (11).

Subsequently, 1 M NaOH was added dropwise to adjust the pH of the reaction mixture to 8.5. This pH adjustment induced the formation of a pale green precipitate, indicating the synthesis of ZnO NPs. The reaction mixture was then allowed to cool to room temperature. The resulting precipitate was collected by filtration, washed several times with deionized water and absolute ethanol to remove any unreacted precursors and residual plant compounds, and then dried in an oven at 60°C for two hours. The dried ZnO NPs were stored in sterile containers for further characterization and biological evaluation.

3.4. Characterization of ZnO Nanoparticles

The ZnO NPs, which were biosynthesized from the rosemary (*S. Rosmarinus*) extract, were characterized by employing analytical techniques to ensure successful formation and to evaluate the physicochemical properties of these nanoparticles in as much detail as possible.

3.4.1. X-Ray Diffraction Analysis

The XRD is instrumental in elucidating the crystalline structure, phase purity, and average crystallite size of synthesized ZnO NPs. In the study, the analysis was carried out using a PANalytical XPert PRO powder X-ray diffractometer with Cu Kα radiation (λ = 1.5406 Å). The ZnO NP powder sample was tightly dried, finely ground to avoid apparent heterogeneity, and then spread evenly on the sample holder (12).

3.4.2. UV-Visible Spectroscopy

UV-Vis spectroscopy confirmed the initial formation of ZnO NPs using rosemary (*S. Rosmarinus*) extract. The absorbance spectra of the UV-Vis used to analyze the nanoparticle suspension were recorded from 200 to 700 nm using a Shimadzu UV-1900 spectrophotometer. The occurrence of characteristic absorption bands, especially in the ultraviolet region, confirms the successful formation of ZnO NPs and provides information about their optical properties (13).

3.4.3. Fourier-Transform Infrared Spectroscopy

To identify the functional groups involved in ZnO NP reduction and stabilization, FTIR spectroscopy was performed using a SHIMADZU 8400 FTIR spectrometer. The spectra were recorded in the mid-infrared region

(4000 - 400 cm^{-1}) at a resolution of 4.0 cm^{-1}. This analysis enabled the identification of phytochemical constituents from the rosemary extract involved in the synthesis of nanoparticles and confirmed the formation of the Zn–O bond (14).

3.4.4. Hydrodynamic Average Size and Zeta Potential Analysis

The hydrodynamic size distribution and surface charge (ZP) of the biosynthesized ZnO NPs were measured using a Malvern Zetasizer instrument. The DLS analysis provided information on average particle size and Polydispersity Index (PDI), while ZP measurements assessed the colloidal stability of the nanoparticle suspension. These two parameters are crucial for evaluating the uniformity and dispersion stability of the synthesized ZnO NPs (15).

3.4.5. Scanning Electron Microscopy and Energy Dispersive X-ray Spectroscopy

Scanning electron microscopy (SEM, MIRA III, Carl Zeiss) was used to analyze the morphology and size of the prepared ZnO NPs. For conductivity enhancement, the dried nanoparticle samples were coated with a thin layer of platinum before imaging. Observations were performed at an accelerating voltage of 4 kV, using higher magnifications (85 KX) to reveal detailed surface features. The EDX was also performed concurrently with SEM to determine the elemental composition and confirm the presence of zinc and oxygen within the nanoparticles, as well as any associated phytochemical residues from the rosemary extract (16).

3.4.6. Antibacterial Activity

The effectiveness of the biosynthesized ZnO NPs, tested for antimicrobial activity using rosemary (*S. Rosmarinus*) extract, was determined by the cup-plate agar diffusion method. Mueller Hinton agar was prepared and poured into sterile petri dishes to solidify at room temperature. Bacterial suspensions of *Staphylococcus aureus* (gram-positive) and *Escherichia coli* (gram-negative) were standardized to a 0.5 McFarland turbidity and evenly spread on the surface of the agar plates using sterile swabs for uniform distribution. Wells in the solidified agar were made with sterile stainless-steel cylinders of 12 mm diameter.

The ZnO NP suspension, prepared in the required concentrations and dissolved in dimethyl sulfoxide (DMSO), was carefully applied into the wells. The positive control consisted of Amoxicillin dissolved in sterile distilled water at concentrations of 100, 50, and 25 μg/mL, while DMSO alone served as the negative control. The plates were incubated at 37°C for 48 hours, after which the diameter of the clear zones of inhibition around each well was measured in millimeters. The sizes of these zones reflected the antibacterial efficacy of ZnO NPs compared to standard antibiotics and the negative control. All tests were performed three times for reliability, and aseptic conditions were maintained throughout to prevent contamination (17).

4. Results and Discussion

4.1. X-Ray Diffraction Analysis

The characteristic peaks of hexagonal wurtzite ZnO (with its reference ICDD card number 36-1451) were observed in the X-ray diffractogram, confirming the phase purity and crystalline nature of the synthesized nanoparticles (Figure 1A). These well-defined and sharp peaks correspond to the (100), (101), (102), (110), (103), (201), and (202) planes (17). The mean crystallite size of the ZnO NPs was found to be 46.14 nm based on XRD analysis, calculated using the Debye-Scherrer equation. This value for the ZnO NPs is either quite similar to or slightly larger than previously reported values in other green synthesis studies, where crystallite sizes typically range from 13 to 51 nm, depending on the plant extract and synthesis conditions employed (18). For example, Alharbi et al. reported ZnO NPs' sizes in the range of 18.77 - 24.39 nm using phytochemical-mediated synthesis, while Begum and Kumuthini observed a size of 51.20 nm for ZnO NPs synthesized via a green route (17, 19).

The increased crystallite size in the present study may, however, be due to the specific phytochemical composition of rosemary extract and the reaction temperature and pH conditions optimized during synthesis.

4.2. UV-Visible Spectroscopy

The UV-Vis spectra results presented in this study compellingly indicate the successful green synthesis of ZnO NPs using rosemary (*S. rosmarinus*) extract. The absorption bands recorded at 200 and 280 nm differ from the absorption peaks generally associated with ZnO NPs synthesized by conventional or other green methods, which typically fall within the range of 320 - 380 nm (5). This blue shift in the absorption spectrum suggests the formation of ultra-small particles, as the optical properties of ZnO NPs are highly size-dependent (Figure 1B). As particle size decreases, quantum confinement effects become more pronounced, leading

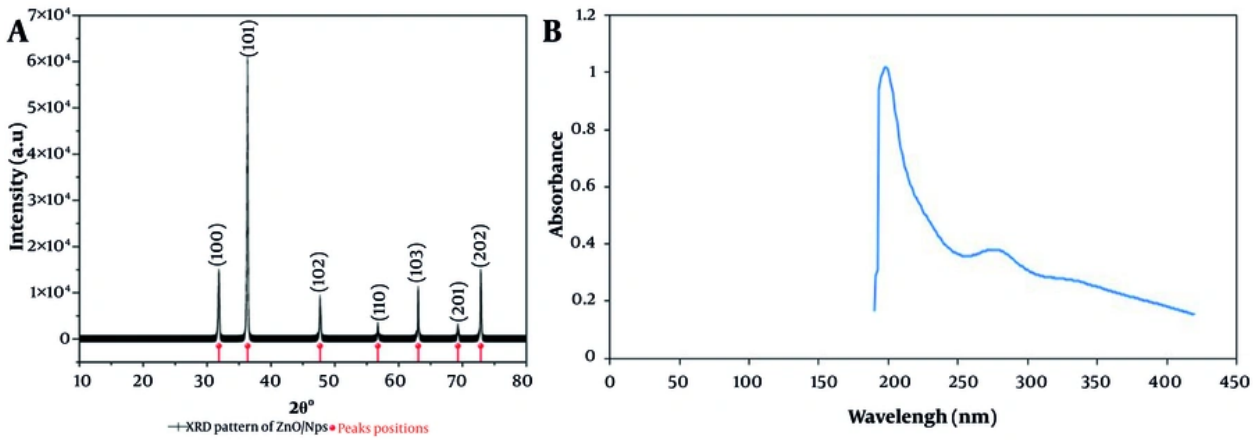

Figure 1. A, X-ray diffraction (XRD) pattern of biosynthesized zinc oxide nanoparticles (ZnO NPs) using rosemary (*Salvia rosmarinus*) extract; B, UV-Visible absorption spectrum of ZnO NPs synthesized with rosemary extract.

to a shift of the absorption band towards shorter wavelengths (higher energy) (20).

The absorption maxima at 200 and 280 nm recorded in this study are indicative of "very small" ZnO NPs, further demonstrated by the sharpness and intensity of peaks, signifying a narrow size distribution and high degree of monodispersity. Recent studies show that ZnO NPs synthesized by rosemary extract generally tend to show absorption maxima in the range of 363 - 370 nm (5). For instance, researchers Uysal et al. found the characteristic absorption peak for rosemary-mediated ZnO NPs to be at 363 nm, attributing it to effective capping and stabilization due to phytochemicals present in the extract (5). Mohanasundaram and Saral also found a blue shift to 363 nm, which they correlated with the formation of ultrasmall monodisperse nanoparticles with modified electronic properties (21).

There is an even greater blue shift in the current study (200 and 280 nm), which strongly indicates the novel synthesis protocol, likely resulting from optimized reaction conditions, extract concentration, or perhaps unique phytochemical interactions specific to the rosemary source used.

4.3. Fourier Transform Infrared Analysis

The FTIR study provides valuable information about the functional groups involved in the green synthesis and stabilization of ZnO NPs using rosemary (*S. rosmarinus*) extract. The FTIR spectrum of rosemary extract displays major absorption bands at 3388, 2935, 1697 - 1417, and 1068 cm^{-1}, corresponding to O–H, C–H, C=O, C=C, and C–O stretching vibrations, respectively (Figure 2A). These bands, characteristic of phytochemicals such as flavonoids, phenolics, and other organic compounds, are abundant in rosemary. This indicates that the extract has a rich phytochemical profile crucial for the reduction and capping of Zn^{2+} ions during nanoparticle synthesis (22).

After forming ZnO NPs, new peaks appear at 475 and 578 cm^{-1} in the FTIR spectra, indicative of Zn-O stretching vibrations (Figure 2B). These peaks are widely recognized as characteristic of ZnO formation and are consistently reported in the literature on green-synthesized ZnO NPs with various plant extracts (23). The FTIR spectra and literature evidence together indicate that rosemary's phenolic repertoire — dominated by rosmarinic acid, carnosic acid, and caffeic acid — drives the green synthesis of nanoparticles. The catechol-type O-phenolic hydroxyl groups in these molecules readily chelate Zn^{2+}, donate electrons via HAT, SET, or SPLET pathways, and reduce the ions to Zn^{0} that subsequently oxidize to crystalline ZnO. Because deprotonation at alkaline pH enhances electron donation, the reduction efficiency rises as synthesis pH increases. After reduction, the same phytochemicals remain adsorbed on the particle surface, supplying steric and electrostatic stabilization that limits agglomeration. Synergistic interplay among multiple phenolics therefore provides both a robust reductive environment and durable organic capping, as confirmed by retained C–O, C=C, and O–H bands

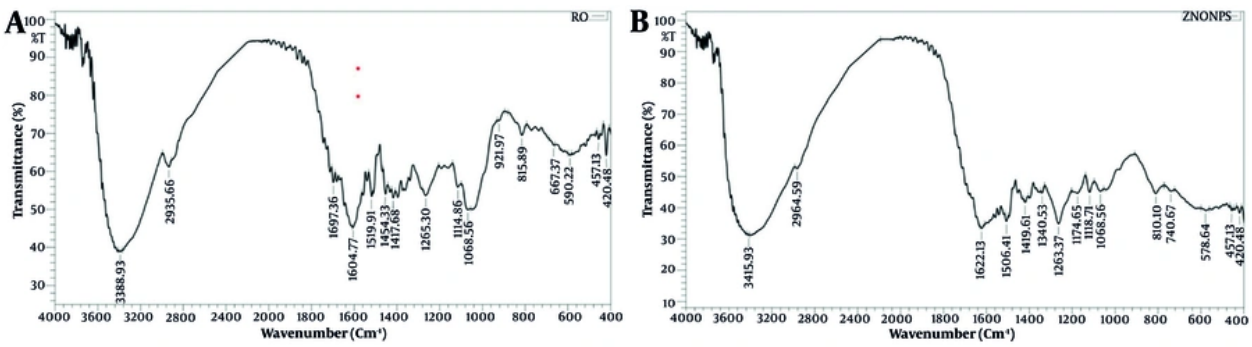

Figure 2. A, Fourier transform infrared (FTIR) spectrum of rosemary (*S. rosmarinus*) extract; B, FTIR spectrum of biosynthesized zinc oxide nanoparticles (ZnO NPs) using rosemary extract.

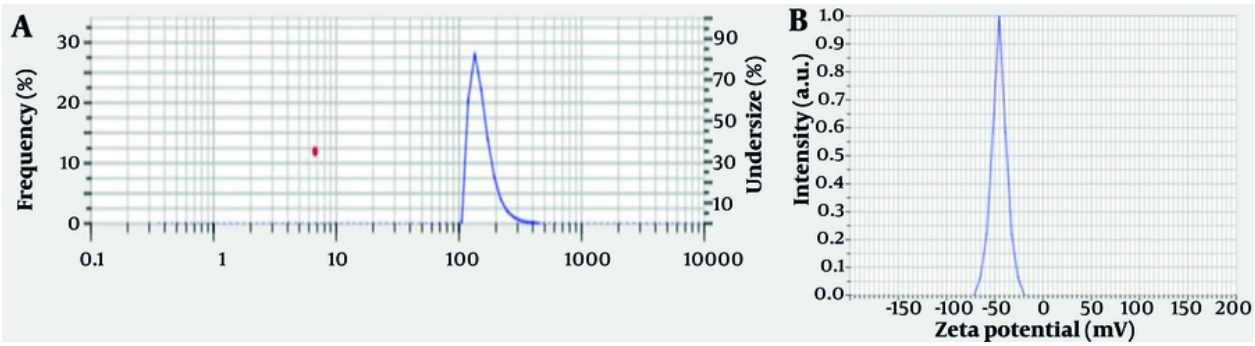

Figure 3. A, dynamic light scattering (DLS) particle size distribution of biosynthesized zinc oxide nanoparticles (ZnO NPs) using rosemary (*Salvia rosmarinus*) extract; B, zeta potential (ZP) analysis of ZnO NPs synthesized with rosemary extract.

alongside Zn–O peaks (475 - 578 cm^{-1}) in the final FTIR profile (24). For example, Uysal et al. demonstrated that ZnO NPs prepared with rosemary exhibit FTIR peaks corresponding to both Zn-O bonds and organic functional groups, confirming the extract's dual role as a reducing and stabilizing agent (5).

Similarly, Aldeen et al. and Suleiman et al. report that the presence of O-H, C=O, and C-O stretching vibrations in FTIR spectra of green-synthesized ZnO NPs indicates phytochemical capping, which enhances nanoparticle stability and biocompatibility (25, 26) Peaks in the 500 to 700 cm^{-1} range are generally accepted as evidence of metal-oxygen bond formation in ZnO NPs, further confirming successful synthesis in this work (27).

4.4. Dynamic Light Scattering Analysis

The DLS analysis provided insights into the colloidal properties and particle size distributions of the biosynthesized ZnO NPs using rosemary (*S. Rosmarinus*) extract. The average hydrodynamic diameter of the ZnO NPs was found to be approximately 652.5 nm with a PDI of 0.471 (Figure 3A). This PDI value indicates a moderately broad size distribution, as values below 0.3 are considered monodisperse, and higher values suggest increased heterogeneity in particle size (28). The size measured is much larger than the primary crystallite size determined by XRD, which is common in DLS measurements due to the technique's sensitivity to agglomerates and the hydrodynamic shell contributed by surface-bound phytochemicals and solvent molecules (29).

Comparative studies have reported sizes ranging widely, even for green-synthesized ZnO NPs measured by

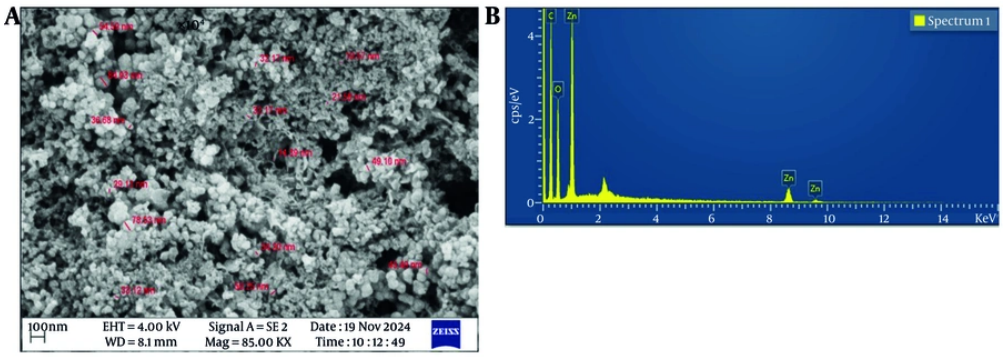

Figure 4. A, scanning electron microscopy (SEM) image of biosynthesized zinc oxide nanoparticles (ZnO NPs) using rosemary (*Salvia rosmarinus*) extract; B, energy-dispersive X-ray spectroscopy (EDX) spectrum of ZnO NPs.

DLS, often influenced by the plant-type extract, synthesis conditions, and degree of aggregation. For example, Abdelbaky et al. reported ZnO NPs synthesized in P. odoratissimum extract as having an average DLS size of 76 nm and a PDI of 0.241, indicating a more uniform distribution (28).

In a counter study, Mohd Yusof et al. reported hydrodynamic diameters of 327.4 ± 634.8 nm for the biosynthesized ZnO NPs, with a PDI of 0.388, illustrating that different green synthesis protocols contribute to variability (29). The greater average size and PDI obtained in the current study may hinge upon the specific phytochemical composition of the rosemary extract, promoting the formation of larger aggregates or clusters within the aqueous suspension.

The ZP measurement is a key parameter for evaluating the colloidal stability of nanoparticle suspensions. In this study, the ZP of the ZnO NPs was measured at about -40 mV, a value well above the ± 30 mV threshold recognized for stable colloidal systems (30). Such a high negative surface charge creates strong electrostatic repulsion between particles, contributing to stabilization against aggregation (Figure 3B). This finding aligns with other reports indicating that green-synthesized ZnO NPs generally display negative ZP s due to the adsorption of phenolic and flavonoid compounds from plant extracts (31). For example, Gonzalez-Fernandez et al. reported a ZP of -29.73 mV for ZnO NPs synthesized from plant extracts, while Yedurkar et al. showed that surface modification could further increase the negative charge and stability of ZnO suspensions (32, 33).

4.5. Morphological Studies

The morphology and elemental characterization of ZnO NPs synthesized from rosemary (*S. Rosmarinus*) extract are comprehensively assessed via SEM and EDX.

The SEM analysis showed that the ZnO NPs were mainly spherical to hexagonal and had relatively uniform morphological and dimensional features (Figure 4A). The nanoparticles appeared as irregular agglomerates with sizes reaching maximum values of almost 100 nm. Such agglomeration is a characteristic feature of green-synthesized ZnO NPs, usually attributed to the presence of phytochemicals from the plant extract acting as reducing and capping agents, which can interfere with and control the nucleation and growth processes during synthesis (34).

The morphological and elemental characterization of ZnO NPs synthesized from rosemary (*S. Rosmarinus*) was thoroughly conducted using SEM and EDX. According to SEM analysis, ZnO NPs were mainly spherical to hexagonal and were highly uniform in morphological and dimensional characteristics. The nanoparticles appeared as irregular aggregates with sizes attaining a maximum value of about 45 nm. Such extreme aggregation is a characteristic feature of green-synthesized ZnO NPs, usually attributed to the presence of phytochemicals from the plant extract that act as both reducing and capping agents, thereby influencing and controlling the nucleation and growth process during synthesis (35).

The reported particle size and morphology align with previous studies on rosemary-mediated green synthesis of ZnO NPs. For example, Biswas et al. (as cited by Al-Hamad et al.) observed that ZnO NPs synthesized using Tecoma stans leaf extract tend to be mostly spherical, with sizes ranging from 15 to 20 nm. Other studies

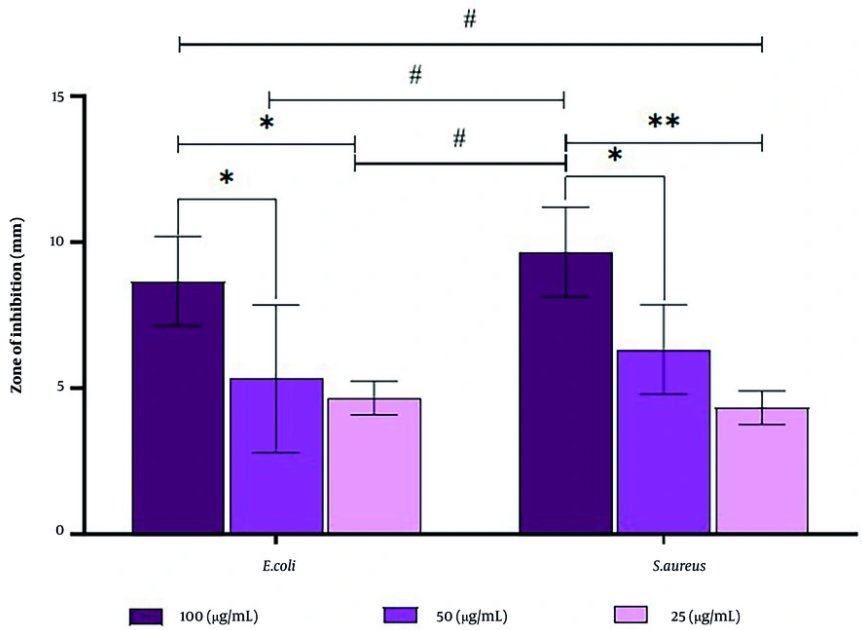

Figure 5. Zone of inhibition (mm) for biosynthesized zinc oxide nanoparticles (ZnO NPs) against *Escherichia coli* and *Staphylococcus aureus* at different concentrations (25, 50, and 100 µg/mL), showing dose-dependent antibacterial activity (values are expressed as mean ± SD; n = 3). The # symbols indicate that for each bacterial strain, increasing the concentration of nanoparticles leads to a statistically significant increase in the zone of inhibition. Furthermore, the * and ** symbols demonstrate a statistically significant difference in susceptibility between the two bacterial strains, showing that *S. aureus* is consistently and significantly more vulnerable to the antibacterial action of the ZnO NPs than E. coli at all tested concentrations.

reported semi-spherical nanoparticles around 18 nm when the rosemary extract concentration was increased from 50 to 75 mL (36, 37). Variations in particle size across different studies likely stem from differences in extract concentration, reaction conditions, and post-synthesis processing. The current study's observations of aggregation may also have contributed to the larger sizes seen in SEM measurements, which often reflect nanoparticle clusters rather than individual crystallites.

The EDX analysis further confirmed the successful synthesis and elemental purity of the ZnO NPs (Figure 4B). The spectrum displayed prominent peaks around 9.6 keV, 8.5 keV, and below 1 keV, corresponding to ZnLα, ZnKα, and ZnKβ, respectively. These peaks are characteristic of zinc and are commonly reported in the literature for green-synthesized ZnO NPs (2). The peak near 0.5 keV indicates the presence of oxygen, confirming ZnO formation. Additionally, the small peak at this energy suggests potential binding of organic compounds from the rosemary extract on the nanoparticle surface, which is typical in plant-mediated synthesis and contributes to improved stability and biocompatibility (38).

4.6. Antibacterial Activity

This study revealed that rosemary-mediated green synthesis of ZnO NPs showed concentration-dependent inhibition in both *E. coli* and *S. aureus*. The mean diameters of inhibition zones tend to increase with a rise in the concentration of ZnO NPs for both organisms under test (Table 1 and Figure 5). For the highest concentration dose (100 µg/mL), there were slightly larger zones of inhibition for *S. aureus* (9.67 ± 1.53 mm) compared to *E. coli* (8.67 ± 1.53 mm). The intermediate and low doses (50 µg/mL and 25 µg/mL) also produced smaller zones of clearance, following the typical dose-response often reported for ZnO systems (5).

At the highest concentration (100 µg/mL), the inhibition zone was much larger than at 25 µg/mL for both bacterial strains ($P \leq 0.0193$). The other significant difference was between the 100 and 50 µg/mL concentrations, which were also significant for *E. coli* and *S. aureus* (identical $P = 0.0495$), thus confirming markedly increasing bactericidal potency above 50 µg/mL. The difference between 25 and 50 µg/mL was not meaningful; non-significant P-values of 0.859 for *E. coli*

Table 1. Zone of Inhibition (mm) for *Escherichia coli* and *Staphylococcus aureus* Treated with Different Concentrations (100, 50, and 25 µg/mL) of Biosynthesized Zinc Oxide Nanoparticles Using Rosemary (*Salvia Rosmarinus*) Extract [a]

Bacterium; Concentration (µg/mL)	Zone (mm)	100 µg/mL vs. 50 µg/mL (P-Value)	100 µg/mL vs. 25 µg/mL (P-Value)	25 µg/mL vs. 50 µg/mL (P-Value)
Escherichia coli				
100	8.67 ± 1.53	0.0495	0.0193	0.859
50	5.33 ± 2.52	-	-	-
25	4.67 ± 0.58	-	-	-
Staphylococcus aureus				
100	9.67 ± 1.53	0.0495	0.0019	0.2827
50	6.33 ± 1.53	-	-	-
25	4.33 ± 0.58	-	-	-

[a] Values are expressed as mean ± SD.

and 0.2827 for *S. aureus* indicate that small sub-MIC increments do not appreciably improve efficacy, a plateau effect consistent with earlier ZnO reports that fail to surpass the threshold needed for effective cell-wall penetration (36).

According to the conclusions of meta-analyses, gram-positive bacteria are always a little bit more susceptible than gram-negative bacteria to ZnO NPs. In line with this, *S. aureus* was more sensitive than *E. coli* at every dose, and that extra 1.00 mm in mean inhibition-zone diameter at 100 µg/mL reached a statistically significant status. This pattern can be explained in terms of structural differences; the large, thick peptidoglycan layer of gram-positive cells facilitates anchoring of the nanoparticle, whereas the thick structure of the gram-negative lipopolysaccharide hinders the entry of the particles (37).

Antibacterial efficacy is certainly correlated to surface area and particle size. Green-synthesized ZnO NPs possess crystallites whose size is generally below 50 nm, creating a large specific surface area through which bacteria make contact in a short time (38). Their small sizes also make them more soluble, leading to the release of Zn^{2+} ions that destabilize membranes and interact with intracellular thiols (39).

It sustains the bactericidal action through reactive oxygen species pathways, which are more developed in both photocatalytic and dark conditions, inducing the generation of hydrogen peroxide and hydroxyl radicals. This leads to lipid peroxidation and protein carbonylation (40). Phytochemicals in rosemary extract create yet another layer of synergy. Compounds like rosmarinic acid, carnosic acid, and essential oils can chelate Zn^{2+} and thereby disrupt the integrity of membranes, causing a reduced energy barrier to the adsorption of nanoparticles while increasing the extent of antimicrobial activity. This effect is most pronounced at the 100 µg/mL concentration 42.

4.7. Conclusions

The present study has efficiently demonstrated the green synthesis of ZnO NPs using rosemary (*S. rosmarinus*) extract as a natural reducing and liquefying agent. The biosynthesized ZnO NPs underwent detailed characterization through a range of analytical techniques such as UV-Vis, FTIR, XRD, DLS, ZP analysis, SEM, and EDX. The results confirm the crystalline formation of phase-pure ZnO NPs in the hexagonal wurtzite structure, with an average crystallite size of 46.14 nm and a hydrodynamic size of 652.5 nm. The nanoparticles exhibited a high negative ZP (-45.4 mV), indicating excellent colloidal stability.

The FTIR and EDX analyses showed that phytochemical residues from the rosemary were attached to the nanoparticle surface, thus highlighting the dual action of the extract in reduction and capping. The SEM images showed predominantly spherical to hexagonal morphologies with the most uniform size distribution, while EDX confirmed the elemental purity of the ZnO NPs. Most importantly, the synthesized ZnO NPs displayed very high antibacterial activity against both gram-positive (*S. aureus*) and gram-negative (*E. coli*) bacteria. Increased bactericidal action, especially against *S. aureus*, is believed to be due to the combined effects of ZnO NPs and phytochemicals originating from rosemary that facilitate disruption of the cell wall and further cause the generation of reactive oxygen species.

This study is novel in utilizing rosemary extract for ecologically synthesized ZnO NPs, resulting in nanoparticles with unique physicochemical and biological properties. This approach eliminates the hazards of chemicals and the energy-consuming processes typically associated with ZnO synthesis, thus

providing a sustainable and scalable route for nanomaterial production. Overall, the findings of this study underscore the potential of plant-mediated green synthesis in producing functional nanomaterials with significant power in antimicrobial therapy, biomedical devices, and environmental remediation. Future investigations should focus on the mechanistic understanding of nanoparticle formation driven by phytochemicals and broaden the application of such green-synthesized ZnO NPs.

Footnotes

Authors' Contribution: N. S. K.: Acquisition of data, analysis, and interpretation of data; D. S. M.: Study concept and design, administrative, technical, material support, and study supervision; S. N. S.: Acquisition of data, analysis, interpretation of data, and statistical analysis; Z. T. A.: Critical revision of the manuscript for important intellectual content and analysis and interpretation of data; F. Q.: Analysis, interpretation of data, study concept, design, and study supervision.

Conflict of Interests Statement: The authors declare no conflict of interest.

Data Availability: The dataset presented in the study is available on request from the corresponding author during submission or after publication.

Ethical Approval: This study is approved under the ethical approval code of S.A/1082 from Misan University, Iraq.

Funding/Support: This research received no funding/support.

References

1. Johari B, Tavangar-Roosta S, Gharbavi M, Sharafi A, Kaboli S, Rezaeejam H. Suppress the cell growth of cancer stem-like cells (NTERA-2) using Sox2-Oct4 decoy oligodeoxynucleotide-encapsulated niosomes-zinc hybrid nanocarriers under X-irradiation. *Heliyon*. 2024;**10**(13). e34096. [PubMed ID: 39071677]. [PubMed Central ID: PMC11277410]. https://doi.org/10.1016/j.heliyon.2024.e34096.
2. Xue Y, bin Ismail AJ, Lansing MG, bin Mohd Hayati MF. Novel green synthesis of zinc oxide nanoparticles using Salvia rosmarinus extract for treatment of human lung cancer. *Open Chem*. 2023;**21**(1). https://doi.org/10.1515/chem-2023-0113.
3. Alhujaily M, Albukhaty S, Yusuf M, Mohammed MKA, Sulaiman GM, Al-Karagoly H, et al. Recent Advances in Plant-Mediated Zinc Oxide Nanoparticles with Their Significant Biomedical Properties. *Bioengineering (Basel)*. 2022;**9**(10). [PubMed ID: 36290509]. [PubMed Central ID: PMC9598103]. https://doi.org/10.3390/bioengineering9100541.
4. Grevsen K, Fretté XC, Christensen LP. Content and composition of volatile terpenes, flavonoids and phenolic acids in Greek oregano (Origanum vulgare L. ssp. hirtum) at different development stages during cultivation in cool temperate climate. *Europ J Horticultural Sci*. 2009;**74**(5):193-203. https://doi.org/10.1079/ejhs.2009/1182840.
5. Uysal Y, Gorkem Dogaroglu Z, Caylali Z, Karakulak DS. Rosemary-Mediated Green Synthesis of ZnO Nanoparticles and their Integration into Hydrogel Matrices: Evaluating Effects on Wheat Growth and Antibacterial Properties. *Glob Chall*. 2024;**8**(11):2400120. [PubMed ID: 39545255]. [PubMed Central ID: PMC11557514]. https://doi.org/10.1002/gch2.202400120.
6. Keshavarz B, Gharbavi M, Bagherpour G, Rezaeejam H, Johari B. Green-Synthesized Silver Nanoparticles Coated with Alginate and Conjugated to Docetaxel Drug: Combination Therapy Under X-Irradiation on LNCaP Prostate Cancer Cells. *J Polymers Environ*. 2025;**33**(7):3029-49. https://doi.org/10.1007/s10924-025-03591-8.
7. Kasem SM, Mahfouz ME, Mira NM, Helal IB. Evaluation of phytochemical profile, antioxidant activity, storage stability, in vitro release kinetics and cytotoxic effects of ultrasonicated Rosmarinus officinalis ethanolic extract and its chitosan-loaded nanoparticles on chicken primary intestinal epithelial cells. *Jokull J*. 2023;**73**:29-68.
8. Shafey AME. Green synthesis of metal and metal oxide nanoparticles from plant leaf extracts and their applications: A review. *Green Proces Synthesis*. 2020;**9**(1):304-39. https://doi.org/10.1515/gps-2020-0031.
9. Adeyemi JO, Oriola AO, Onwudiwe DC, Oyedeji AO. Plant Extracts Mediated Metal-Based Nanoparticles: Synthesis and Biological Applications. *Biomolecules*. 2022;**12**(5). [PubMed ID: 35625555]. [PubMed Central ID: PMC9138950]. https://doi.org/10.3390/biom12050627.
10. Gharbavi M, Johari B, Tabar RM, Sharafi A. Selenium-doped albumin nanoparticles enhance tamoxifen-induced anticancer effects in 4T-1 mouse breast cancer cells. *Appl Organometallic Chem*. 2023;**38**(2). https://doi.org/10.1002/aoc.7327.
11. Hassanpouraghdam MB, Mehrabani LV, Tzortzakis N. Foliar Application of Nano-zinc and Iron Affects Physiological Attributes of Rosmarinus officinalis and Quietens NaCl Salinity Depression. *J Soil Sci Plant Nutrition*. 2019;**20**(2):335-45. https://doi.org/10.1007/s42729-019-00111-1.
12. Ghaffarlou M, Rashidzadeh H, Mohammadi A, Mousazadeh N, Barsbay M, Sharafi A, et al. Photothermal and radiotherapy with alginate-coated gold nanoparticles for breast cancer treatment. *Sci Rep*. 2024;**14**(1):13299. [PubMed ID: 38858410]. [PubMed Central ID: PMC11164878]. https://doi.org/10.1038/s41598-024-60396-w.
13. Rashidzadeh H, Gharbavi M, Ghorbani R, Nazari M, Noei H, Johari B. Co-Encapsulated Niosomes With Metformin and Silver Nanoparticles as Potential Anticancer Tool for the Combined Therapy on Lung Cancer Cells. *Appl Organometallic Chem*. 2025;**39**(7). https://doi.org/10.1002/aoc.70279.
14. Heidari S, Gharbavi M, Ghorbani R, Rezaeejam H, Johari B. Combined treatment using bismuth sulfide nanoparticles loaded with NANOG decoy oligodeoxynucleotides under X-ray radiation for breast cancer cells. *Sci Rep*. 2025;**15**(1):23131. [PubMed ID: 40594465]. [PubMed Central ID: PMC12219885]. https://doi.org/10.1038/s41598-025-05074-1.
15. Aghapur N, Gharbavi M, Bigdelou Z, Zand M, Johari B. Green synthesis of silver nanoparticles coated with methotrexate-conjugated polyvinyl alcohol: As potential nanosystem for chemo/radiotherapy. *J Drug Delivery Sci Technol*. 2025;**105**. https://doi.org/10.1016/j.jddst.2025.106643.
16. Asadi N, Gharbavi M, Rezaeejam H, Farajollahi A, Johari B. Zinc nanoparticles coated with doxorubicin-conjugated alginate as a radiation sensitizer in triple-negative breast cancer cells. *Int J Pharm*. 2024;**659**:124285. [PubMed ID: 38821433]. https://doi.org/10.1016/j.ijpharm.2024.124285.

17. Begum S, Kumuthini R. Characterization of zinc oxide nano particles synthesized via chemical and green method. *Ovonic Res*. 2023;**19**(5):505-12.
18. Saryanto H, Sebayang D. The simple fabrication of nanorods mass production for the dye-sensitized solar cell. *MATEC Web of Conferences*. EDP Sciences; 2017. 3006 p.
19. Alharbi FN, Abaker ZM, Makawi SZA. Phytochemical Substances—Mediated Synthesis of Zinc Oxide Nanoparticles (ZnO NPS). *Inorganics*. 2023;**11**(8). https://doi.org/10.3390/inorganics11080328.
20. Alprol AE, Eleryan A, Abouelwafa A, Gad AM, Hamad TM. Green synthesis of zinc oxide nanoparticles using Padina pavonica extract for efficient photocatalytic removal of methylene blue. *Sci Rep*. 2024;**14**(1):32160. [PubMed ID: 39741157]. [PubMed Central ID: PMC11688442]. https://doi.org/10.1038/s41598-024-80757-9.
21. Mohanasundaram P, Saral AM. Binding properties and biological applications of green synthesized ZnO nanoparticles from neem flower. *Sci Rep*. 2025;**15**(1):17727. [PubMed ID: 40399393]. [PubMed Central ID: PMC12095587]. https://doi.org/10.1038/s41598-025-02157-x.
22. Kaur H, Kumar S, Bouzid G. Exploring the role of different phytochemicals on the morphological variations of metal and metal oxide nanomaterials for biomedical application. *Interactions*. 2024;**245**(1). https://doi.org/10.1007/s10751-024-02088-5.
23. El-Belely EF, Farag MMS, Said HA, Amin AS, Azab E, Gobouri AA, et al. Green Synthesis of Zinc Oxide Nanoparticles (ZnO-NPs) Using Arthrospira platensis (Class: Cyanophyceae) and Evaluation of their Biomedical Activities. *Nanomaterials (Basel)*. 2021;**11**(1). [PubMed ID: 33406606]. [PubMed Central ID: PMC7823323]. https://doi.org/10.3390/nano11010095.
24. Elsehemy MS, Monam YK, Galhoum AA, Bayoumi EE, Gado WS, El-Khair MA, et al. Synthesis, Characterization, and Evaluation of Zero-Valent Iron Nanoparticles from Different Leaf Extracts: Photo-Catalytic Dibenzothiophene Degradation and Antimicrobial Efficiency. *Chem Select*. 2025;**10**(15). https://doi.org/10.1002/slct.202403785.
25. Aldeen TS, Ahmed Mohamed HE, Maaza M. ZnO nanoparticles prepared via a green synthesis approach: Physical properties, photocatalytic and antibacterial activity. *J Physics Chem Solids*. 2022;**160**. https://doi.org/10.1016/j.jpcs.2021.110313.
26. Suleiman MH, El-Sheikh SM, Mohamed ET, El Raey MA, El Sherbiny S, Morsy FA, et al. Green synthesis of ZnO-NPs using sugarcane bagasse waste: phytochemical assessment of extract and biological study of nanoparticles. *Dalton Trans*. 2024;**53**(46):18494-505. [PubMed ID: 39474919]. https://doi.org/10.1039/d4dt02449d.
27. Raha S, Ahmaruzzaman M. ZnO nanostructured materials and their potential applications: progress, challenges and perspectives. *Nanoscale Adv*. 2022;**4**(8):1868-925. [PubMed ID: 36133407]. [PubMed Central ID: PMC9419838]. https://doi.org/10.1039/d1na00880c.
28. Abdelbaky AS, Abd El-Mageed TA, Babalghith AO, Selim S, Mohamed A. Green Synthesis and Characterization of ZnO Nanoparticles Using Pelargonium odoratissimum (L.) Aqueous Leaf Extract and Their Antioxidant, Antibacterial and Anti-inflammatory Activities. *Antioxidants (Basel)*. 2022;**11**(8). [PubMed ID: 35892646]. [PubMed Central ID: PMC9329751]. https://doi.org/10.3390/antiox11081444.
29. Mohd Yusof H, Abdul Rahman N, Mohamad R, Zaidan UH, Samsudin AA. Biosynthesis of zinc oxide nanoparticles by cell-biomass and supernatant of Lactobacillus plantarum TA4 and its antibacterial and biocompatibility properties. *Sci Rep*. 2020;**10**(1):19996. [PubMed ID: 33204003]. [PubMed Central ID: PMC7673015]. https://doi.org/10.1038/s41598-020-76402-w.
30. Kim KM, Choi MH, Lee JK, Jeong J, Kim YR, Kim MK, et al. Physicochemical properties of surface charge-modified ZnO nanoparticles with different particle sizes. *Int J Nanomedicine*. 2014;**9 Suppl 2**(Suppl 2):41-56. [PubMed ID: 25565825]. [PubMed Central ID: PMC4279853]. https://doi.org/10.2147/IJN.S57923.
31. Hussain RT, Hossain MS, Shariffuddin JH. Green synthesis and photocatalytic insights: A review of zinc oxide nanoparticles in wastewater treatment. *Materials Today Sustainability*. 2024;**26**. https://doi.org/10.1016/j.mtsust.2024.100764.
32. Gonzalez-Fernández JV, Pinzón-Moreno DD, Neciosup-Puican AA, Carranza-Oropeza MV. Green method, optical and structural characterization of ZnO nanoparticles synthesized using leaves extract of M. oleifera. *J Renewable Materials*. 2022;**10**(3):833.
33. Yedurkar S, Maurya C, Mahanwar P. Biosynthesis of Zinc Oxide Nanoparticles Using Ixora Coccinea Leaf Extract—A Green Approach. *Open J Synthesis Theory Appl*. 2016;**5**(1):1-14. https://doi.org/10.4236/ojsta.2016.51001.
34. Habeeb T, Aljohani MS, Kebeish R, Al-Badwy A, Bashal AH. Biogenic synthesis of CoO and ZnO nanoparticles using rosemary extract: Synergistic antimicrobial activity and insights from DFT simulations. *J Mol Structure*. 2024;**1313**. https://doi.org/10.1016/j.molstruc.2024.138714.
35. Faisal S, Jan H, Shah SA, Shah S, Khan A, Akbar MT, et al. Green Synthesis of Zinc Oxide (ZnO) Nanoparticles Using Aqueous Fruit Extracts of Myristica fragrans: Their Characterizations and Biological and Environmental Applications. *ACS Omega*. 2021;**6**(14):9709-22. [PubMed ID: 33869951]. [PubMed Central ID: PMC8047667]. https://doi.org/10.1021/acsomega.1c00310.
36. Pitjamit S, Vichiansan N, Leksakul K, Boonyawan D. Optimization of Ultrasonic and Microbubble Disinfection for Escherichia coli and Staphylococcus aureus: Experimental Design and Effectiveness Evaluation. *J Engin Technol Sci*. 2024;**56**(6):742-55. https://doi.org/10.5614/j.eng.technol.sci.2024.56.6.6.
37. Al-Hamad KA, Asiri A, Alqahtani AM, Alotaibi S, Almalki A. Monitoring the Antibacterial Activity of the Green Synthesized ZnO Nanoparticles on the Negative and Positive Gram Bacteria Mimicking Oral Environment by Using a Quartz Tuning Fork (QTF) Micromechanical Sensor. *Int J Nanomedicine*. 2025;**20**:7975-85. [PubMed ID: 40599395]. [PubMed Central ID: PMC12209601]. https://doi.org/10.2147/IJN.S480164.
38. Babayevska N, Przysiecka L, Iatsunskyi I, Nowaczyk G, Jarek M, Janiszewska E, et al. ZnO size and shape effect on antibacterial activity and cytotoxicity profile. *Sci Rep*. 2022;**12**(1):8148. [PubMed ID: 35581357]. [PubMed Central ID: PMC9114415]. https://doi.org/10.1038/s41598-022-12134-3.
39. Albarakaty FM, Alzaban MI, Alharbi NK, Bagrwan FS, Abd El-Aziz AR, Mahmoud MA. Zinc oxide Nanoparticles, Biosynthesis, characterization and their potent photocatalytic degradation, and antioxidant activities. *J King Saud Univ-Sci*. 2023;**35**(1). https://doi.org/10.1016/j.jksus.2022.102434.
40. Slman AA. Antibacterial activity of Zno nanoparticle on some gram-positive and gram-negative bacteria. *Iraqi J Physics*. 2012;**10**(18):5-10.